

# Structure and Stability of Salicylic Acid–Water Complexes and the Effect of Molecular Hydration on the Spectral Properties of Salicylic Acid

Ashwani Kumar Tiwari and N. Sathyamurthy\*

Department of Chemistry, Indian Institute of Technology Kanpur, Kanpur 208016, India

Received: February 9, 2006; In Final Form: March 8, 2006

Density functional theory with B3LYP parametrization and 6-311++G(d,p) basis set has been used to investigate the structure and stability of salicylic acid–water complexes. The vertical excitation energies for these complexes have been computed using time-dependent density functional theory (with B3LYP parametrization and a 6-311++G(d,p) basis set). It is shown that the hydrogen bond between the carboxylic hydrogen and the oxygen of water is the strongest among all possible hydrogen bonds in the system. The hydrogen bond strength in salicylic acid–water complexes seems to be nearly additive. The change in absorption maximum ( $\lambda_{\text{max}}$ ) corresponding to the vertical excitation energy for the first three excited singlet and triplet states of the complex with 1–3 water molecules is nominal ( $\sim 1$ –3 nm). But with the addition of the fourth water molecule, the  $\lambda_{\text{max}}$  for  $S_1$  and  $T_1$  decreases by  $\sim 17$  nm and it increases for  $S_2$  and  $S_3$  by about the same amount. The decrease in  $\lambda_{\text{max}}$  for transition to the  $T_2$  state on the addition of the fourth water molecule is only  $\sim 9$  nm. There seems to be an intersystem crossing between the  $S_1$  and  $T_3$  states that could account for the observed fluorescence quenching of salicylic acid in water.

## Introduction

The photophysics of salicylic acid (SA) has been studied extensively because of the possibility of excited-state proton transfer (ESIPT).<sup>1–21</sup> Weller<sup>1</sup> pointed out the dual emission in the fluorescence spectrum of salicylic acid and methyl salicylate and attributed it to the asymmetric double-well potentials arising from proton transfer in the ground state and also in the excited state. Pant and co-workers<sup>2–4</sup> investigated the photophysics and photochemistry of salicylic acid extensively using steady-state and time-resolved spectroscopy techniques. They reported that a dilute solution of salicylic acid in alkanes emits at 450 nm, whereas, in a concentrated solution and in solid state, its dimer shows two emissions, one at 370 nm and another at 450 nm. They attributed the emission from the dilute solution to the intramolecular proton transfer and from the concentrated solution and solid state to double proton transfer and tunneling in the excited state. They also studied the spectral properties of salicylic acid in the presence of acids, bases, alcohols, and ethers. The emission from an alcoholic medium such as methanol was attributed to the zwitterion and monoanion of SA. The addition of a small amount of an acid resulted only in zwitterionic emission, whereas the addition of a small amount of alkali led to emission from the monoanion of SA. In concentrated sulfuric acid solution, emission from protonated SA was observed, whereas, in concentrated potassium hydroxide solution, the dianion of SA was the emitting species. In hydrogen-bonding solvents like diethyl ether, hydrogen-bonded monomers were present. In poly(methyl methacrylate) matrix, only the monomeric emission was observed. The deactivation of the cation was found to be similar to that of the zwitterion, indicating that the presence of an extra proton in the carboxylic group increased the nonradiative process. Hydrogen bonding and viscosity/rigidity of the matrix had also been found to decrease the deactivation rate in zwitterions.

Bisht et al. investigated the excited-state enol–keto tautomerization in salicylic acid under supersonic free jet expansion

conditions<sup>5</sup> and the effect of high pressure on it by steady-state absorption and fluorescence measurements.<sup>6</sup> In the jet expansion study, they found that, of the two possible rotamers of salicylic acid, only one rotamer in which the carbonyl oxygen is hydrogen bonded to phenolic hydrogen shows enol–keto tautomerism in the excited state and therefore its emission spectra contained two components, normal UV and tautomer blue. The other rotamer, which does not show excited-state tautomerization, emits only in UV. With the help of steady-state absorption and fluorescence measurements, they showed that, in dilute solution, the emission intensity of the keto form of the monomer increased with increasing pressure. Yahagi et al.<sup>7</sup> found experimentally that intramolecular hydrogen-bonded OH stretching vibrations of the monomer changed drastically upon electronic transition. They did not find any evidence for intermolecular double proton transfer in the ground state as well as the first excited singlet state of the dimer. Sobolewski and Domcke<sup>8</sup> studied excited-state intramolecular proton dislocation (they preferred to use the word dislocation rather than transfer) using *ab initio* quantum chemical methods. Their configuration interaction single excitation (CIS) calculations predicted a single minimum on the first excited singlet state ( $S_1$ ) surface rather than two (enol and keto) minima found in earlier semiempirical (AM1) calculations. Therefore, they concluded that the photophysics of salicylic acid was better described by excited-state vibrational relaxation rather than proton transfer. They also predicted that most of the Stokes shift in the observed fluorescence arose from the rearrangement of the hydrogen-chelating ring.

Maheshwari et al.<sup>9</sup> investigated the ground and excited states of salicylic acid at the RHF(CIS)/6-31G(d,p) and AM1 levels of theory. They obtained a single minimum in the ground-state potential energy curve for intramolecular proton transfer and two minima in the first excited singlet state potential energy curve and thereby accounted for the dual emission in salicylic acid. They also accounted qualitatively for the change in spectral properties with change in pH of the solution. Sobolewski and Domcke<sup>10</sup> studied the excited-state geometries and vibrational

\* Corresponding author. E-mail: nsath@iitk.ac.in.

spectra of anthranilic acid and salicylic acid using time-dependent density functional theory at the B3LYP level of parametrization. They found a single minimum in the  $S_1$  state potential energy surface rather than separate enol–keto minima. The excited-state minimum corresponded to a shortening of the intramolecular hydrogen bond by 0.322 Å. A large red shift of 1400  $\text{cm}^{-1}$  and a strong mixing with H-chelate ring bending and stretching motions was predicted for phenolic OH stretching vibration in the  $S_1$  state by their calculations. Mitsuzuka et al.<sup>11</sup> observed OH stretching vibration of methyl salicylate and its solvated clusters in a supersonic free jet using fluorescence-detected infrared spectroscopy. The OH band of methyl salicylate was weak and broad because of intramolecular hydrogen bond. On the basis of their experiment, they also inferred that the intramolecular hydrogen bond in SA is retained in clusters of ammonia, methanol, and water. They found an opposite behavior in the direction of the electronic transition frequency shift and the OH stretching frequency shift between the clusters with acidic (water and methanol) and basic (ammonia) solvents.

Lahmani and Zehnacker-Rentien<sup>12</sup> investigated the jet-cooled heterodimers of salicylic acid with acetic acid and trifluoroacetic acid in a supersonic expansion. The fluorescence excitation spectra were characterized by a long harmonic progression for a low-frequency mode, and their origin was blue-shifted with respect to that of pure salicylic acid. The emission spectra exhibited a single broad band peaking at 360 and 390 nm for the complex with trifluoroacetic acid and acetic acid, respectively and were independent of the excitation wavelength. They rationalized the results in terms of a single minimum energy curve for both the ground and the excited states. El-Nasr et al.<sup>13</sup> studied the effect of substitution on ESIPT of salicylic acid taking 5-methoxysalicylic acid as a model compound. They found that the electronic absorption and emission spectra of the substituted compound showed a mirror-image relation between the two, an indication of the suppression of excited-state intramolecular proton transfer.

Study of intermolecular hydrogen bonds between salicylic acid and water molecules is important to understand the effect of hydration on the properties of salicylic acid. El-Nasr et al.<sup>14</sup> have investigated the spectral properties of salicylic acid complexed with one water molecule using laser spectroscopic techniques and quantum chemical methods. They found that intramolecular excited-state proton dislocation in salicylic acid is hardly affected by interaction with one water molecule. Mishra et al.<sup>15</sup> studied photoluminescence of salicylic acid and its sodium salt in poly(vinyl alcohol) film and its quenching by water using steady-state and time domain fluorescence measurements. They showed that with increasing percentage of water (in the solution in which the film is immersed), the fluorescence intensity decreases. The mechanism of fluorescence quenching in salicylic acid by water has not been understood so far. Therefore, a time-dependent density functional theoretic (TD-DFT) study of the electronic excited states of salicylic acid–water complexes was undertaken by us.

All ground-state geometries have been optimized using density functional theory, with B3LYP parametrization<sup>22</sup> and basis set 6-311++G(d,p), using the Gaussian 03 suite of programs.<sup>23</sup> The vertical excitation energies for salicylic acid have been computed using TDDFT methodology with the same B3LYP parametrization and 6-311++G(d,p) basis set. Stabilization energies ( $\Delta E_{\text{stab}}$ ) of the salicylic acid–water complexes have been calculated as follows:

$$\Delta E_{\text{stab}} = E_{\text{complex}} - (E_{\text{salicylic acid}} + \sum_n E_{\text{water}}^n) \quad (1)$$

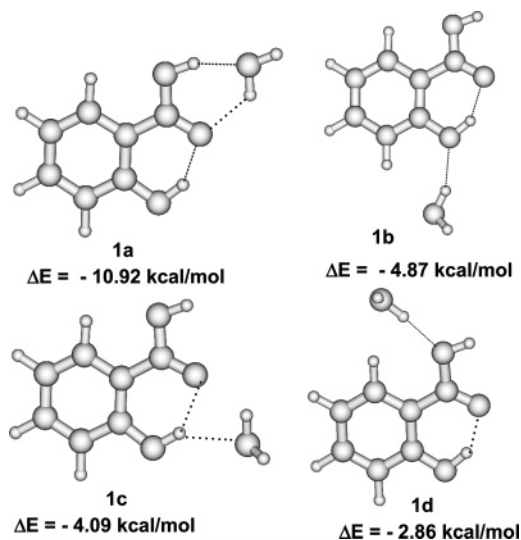


**Figure 1.** Structure and stability of SA– $W_1$  complexes. The large spheres represent carbon and oxygen atoms, while the small spheres represent the hydrogen atoms. Hydrogen bonds are indicated by dotted lines.

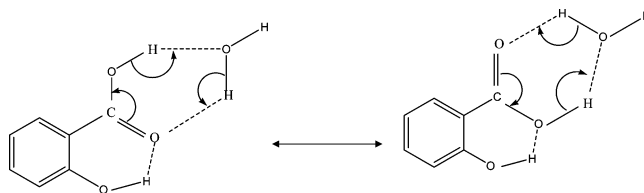


**Figure 2.** Resonance-assisted hydrogen bonds in complex 1a.

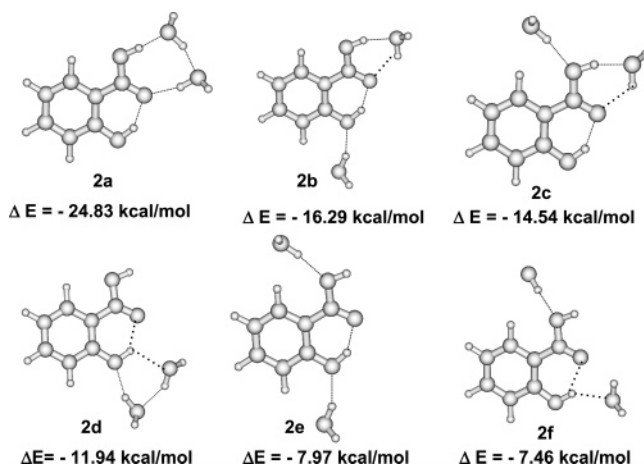


**Figure 3.** Same as Figure 1 for SA– $W_2$  complexes.

Here  $n$  is the number of water molecules present in the complex.  $E_{\text{salicylic acid}}$  and  $E_{\text{water}}^n$  refer to the energies of the respective molecules in the geometry of the complex. The stabilization energies were corrected for basis set superposition error using the method of Boys and Bernardi.<sup>24</sup>

## Results and Discussion

The structures of different possible isomers of salicylic acid–water (SA– $W_n$ ) complexes, with  $n = 1–3$ , as obtained from DFT calculations are presented in Figures 1, 3, and 4, respectively, along with their stabilization energies. That they are indeed true minima has been verified by frequency calculations. Four different initial geometries for the SA– $W_1$  complex, in the vicinity of the three different oxygen atoms and the carboxylic hydrogen, led to the different stable geometries

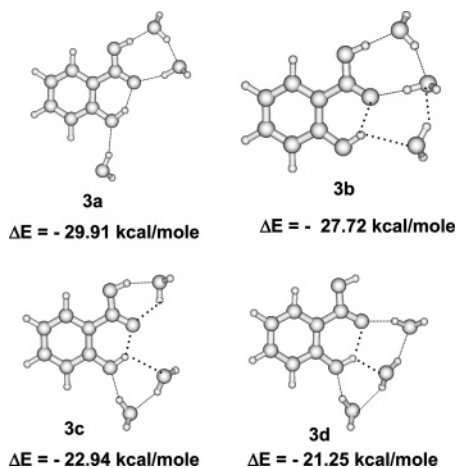


**Figure 4.** Same as Figure 1 for SA–W<sub>3</sub> complexes.

depicted in Figure 1. The isomer 1a is much more stable than the three other isomers of SA–W<sub>1</sub>. The larger stabilization energy for isomer 1a arises from the additional stability of the cyclic structure with two resonating hydrogen bonds,<sup>25</sup> as illustrated in Figure 2. In isomer 1a, both salicylic acid and water act as acceptors as well as donors. The stabilization energy for 1a is  $-10.06$  kcal/mol (BSSE corrected), which is nearly equal to the stabilization energy of a similar isomer of formic acid–water (FA–W<sub>1</sub>) complex ( $-10.38$  kcal/mol), obtained at the same level of theory.<sup>26</sup> The two intermolecular hydrogen bond distances in isomer 1a are  $1.77$  Å (carboxylic group acts as the hydrogen donor) and  $2.07$  Å (water acts as the hydrogen donor). In FA–W<sub>1</sub> these distances are  $1.79$  and  $2.03$  Å, respectively.<sup>26</sup> Comparable stabilization energy and hydrogen bond distances for similar isomers of SA–W<sub>1</sub> and FA–W<sub>1</sub> indicate that the phenol moiety has little effect on the hydrogen bonding between the carboxylic moiety and the water molecule. Our results are in agreement with the experimental findings of El-Nasr et al.<sup>14</sup>

To obtain the most stable geometry for the SA–W<sub>2</sub> complex, different initial geometries were tried and they all led to six different isomers as illustrated in Figure 3. They can be classified in two groups: (i) three isomers (2a–c) in which water is cyclically hydrogen bonded to the carboxylic moiety and (ii) three isomers (2d–f) in which water is *not* cyclically bonded to the carboxylic moiety. Members of the first group are more stable than the members of the second. This indicates that a cyclic hydrogen bond between the carboxylic moiety and water molecules is preferred over an open chain hydrogen bond between the phenolic oxygen/hydrogen and water's hydrogen/oxygen. Further, the isomer 2a in which both the water molecules are cyclically hydrogen bonded to the carboxylic moiety is the most stable.

By addition of one more water molecule to each of the six different structures for SA–W<sub>2</sub>, four different isomers of SA–W<sub>3</sub> were obtained as shown in Figure 4. Isomers 3a,b in which two water molecules form cyclic structures with the carboxylic moiety are more stable than the other two isomers 3c (only one water molecule forms a cyclic structure) and 3d (no cyclic structure with carboxylic OH). The order of stability is  $3a > 3b > 3c > 3d$ . On examination of all possible isomers of SA–W<sub>1</sub>, SA–W<sub>2</sub>, and SA–W<sub>3</sub>, it is clear that resonance-assisted hydrogen bonds between carboxylic moiety and water molecules have a larger stabilizing effect than other hydrogen bonds.

Stabilization energies of different isomers of SA–W<sub>1</sub>, SA–W<sub>2</sub>, and SA–W<sub>3</sub> indicate clearly the additivity of hydrogen bond strength. The hydrogen bond in isomers 2b–f can be considered

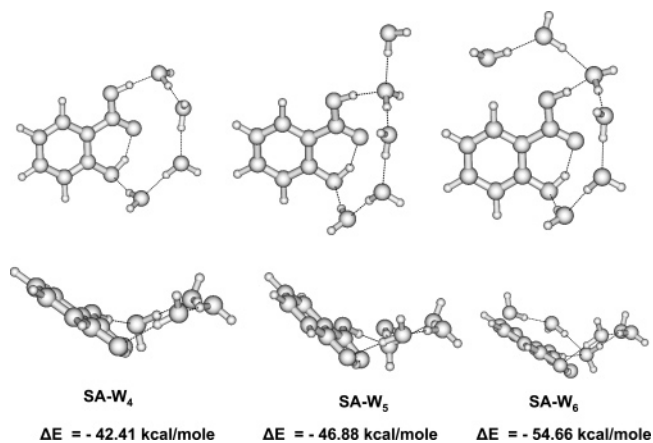


**Figure 5.** Same as Figure 1 for geometry-optimized SA–W<sub>n</sub> ( $n = 4–6$ ) complexes. The side view is also shown in each case to illustrate the open-book structure.

**TABLE 1: Stabilization Energies of Salicylic Acid–Water Complexes Computed by DFT(B3LYP)/6-311++G(d,p) Methodology**

complex	$\Delta E_{\text{stab}}$ (kcal/mol)	$\Delta E_{\text{stab}}$ (BSSE corrected) (kcal/mol)
SA–W <sub>1a</sub>	–10.92	–10.06
SA–W <sub>1b</sub>	–4.87	–4.32
SA–W <sub>1c</sub>	–4.09	–3.42
SA–W <sub>1d</sub>	–2.86	–2.33
SA–W <sub>2a</sub>	–24.83	–22.52
SA–W <sub>2b</sub>	–16.29	–14.63
SA–W <sub>2c</sub>	–14.54	–12.87
SA–W <sub>2d</sub>	–11.94	–9.93
SA–W <sub>2e</sub>	–7.97	–6.50
SA–W <sub>2f</sub>	–7.46	–6.11
SA–W <sub>3a</sub>	–29.91	–27.02
SA–W <sub>3b</sub>	–27.72	–24.69
SA–W <sub>3c</sub>	–22.94	–20.24
SA–W <sub>3d</sub>	–21.25	–18.67
SA–W <sub>4</sub>	–42.41	–37.66
SA–W <sub>5</sub>	–46.88	–41.67
SA–W <sub>6</sub>	–54.66	–46.90

as the combination of hydrogen bonds in the pairs 1a,b, 1a,d, 1b,c, 1b,d, and 1c,d, respectively. For example, the sum of the stabilization energy of 1a ( $-10.06$  kcal/mol) and 1b ( $-4.32$  kcal/mol) is  $-14.36$  kcal/mol,  $0.27$  kcal/mol higher than the stabilization energy of 2b ( $-14.63$  kcal/mol). Similarly, the sum of the stabilization energy of 1a ( $-10.06$  kcal/mol) and 1c ( $-3.42$  kcal/mol) is  $-13.46$  kcal/mol,  $0.49$  kcal/mol lower than the stabilization energy of 2c ( $-12.87$  kcal/mol). It is clear from Table 1 that the stabilization energies of other isomers of SA–W<sub>2</sub> are also nearly equal to the sum of the stabilization energies of the contributing isomers of SA–W<sub>1</sub>. Similarly the hydrogen bonds in 3a–c can be considered as the combination of hydrogen bonds in the pairs 2a,1b, 2a,1c, and 2d,1a, respectively.

Addition of one water molecule to each of the four possible structures for SA–W<sub>3</sub> in Figure 4 led to the structure shown in Figure 5. Similar exercise led to the most stable geometries for SA–W<sub>5</sub> and SA–W<sub>6</sub> illustrated in Figure 5. In contrast to the planar geometry of SA–W<sub>n</sub>,  $n = 1–3$  complexes, SA–W<sub>4</sub> is an open-book-like structure in which four water molecules form a hydrogen-bonded ring, which is at an angle with respect to the molecular plane of salicylic acid. It is also clear that, with four water molecules, the first solvation shell of salicylic acid is filled. The ring structure of water molecules obtained in SA–W<sub>4</sub> is retained in SA–W<sub>5</sub> and SA–W<sub>6</sub>. The additional water molecules in SA–W<sub>5</sub> and SA–W<sub>6</sub> get attached to the ring structure of SA–W<sub>4</sub> as a branched chain, keeping the open-book structure intact.



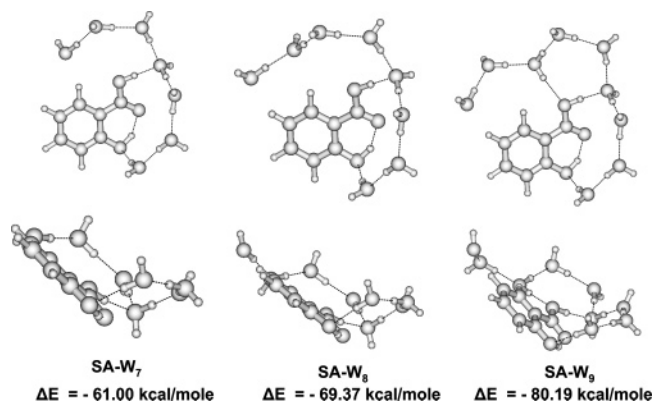


**Figure 6.** Same as Figure 1 for optimized geometry for SA- $W_n$  ( $n = 7-9$ ) complexes.

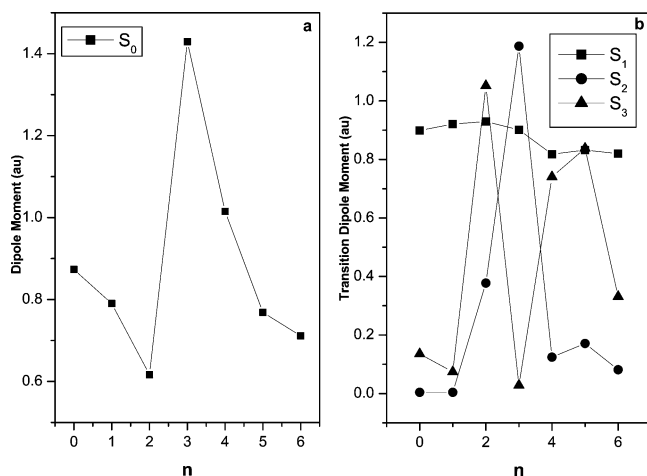


**Figure 7.** Dependence of (a) dipole moment for the ground state and (b) the transition dipole moment for the excited states on the number of water molecules in the complex.

**TABLE 2: Dipole Moment of the Ground ( $S_0$ ) State and the Transition Dipole Moment for  $S_1$ ,  $S_2$ , and  $S_3$  States of Salicylic Acid–Water Complexes in Atomic Units**

complex	$S_0$	$S_1$	$S_2$	$S_3$
SA	0.8733	0.8990	0.0042	0.1356
SA- $W_{1a}$	0.7902	0.9208	0.0042	0.0740
SA- $W_{2a}$	0.6167	0.9296	0.3775	1.0519
SA- $W_{3a}$	1.4295	0.9013	1.1870	0.0282
SA- $W_4$	1.0150	0.8180	0.1244	0.7405
SA- $W_5$	0.7685	0.8321	0.1710	0.8379
SA- $W_6$	0.7113	0.8198	0.0814	0.3314

It is worth pointing out that as more and more water molecules are added to the SA- $W_n$  complex, the clustering takes place at the hydrophilic (carboxyl and phenolic) side and not the hydrophobic side. This is also clear from the optimized geometries of SA- $W_n$ ,  $n = 7-9$ , illustrated in Figure 6.

The dipole moment of the ground state and the transition dipole moment for the excited states of SA- $W_n$  complexes are plotted as a function of the number of water molecules ( $n$ ) in the complex in Figure 7a,b, respectively. The dipole moment of the ground state decreases with increase in the number of water molecules up to  $n = 2$  (Table 2). Further addition of a water molecule increases the dipole moment dramatically, and then the dipole moment starts decreasing with further increase in  $n$ . Close examination of the values reveals that this is purely a consequence of the vector addition of the individual molecular dipole moments in the optimized geometry. The transition dipole moment values for the first excited singlet state ( $S_1$ ) remains approximately constant for  $n = 0-3$ . Addition of the fourth

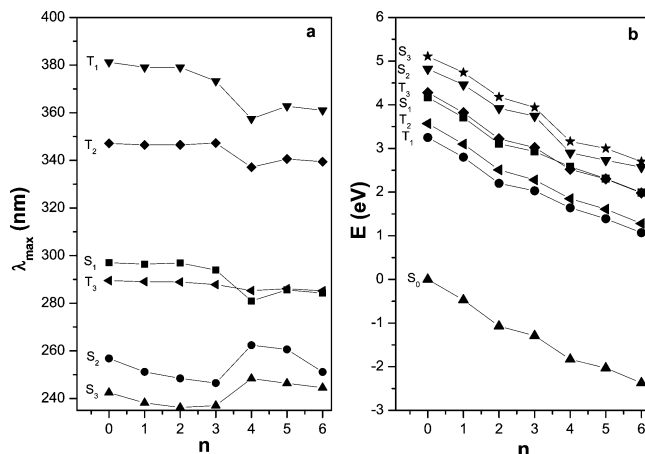


**Figure 8.** Plot of (a) absorption maximum value and (b) energy relative to the ground state of salicylic acid for the different singlet and triplet excited states of SA- $W_n$  complexes as a function of the number of water molecules present.

water molecule to the SA- $W_3$  complex decreases the transition dipole moment (for  $S_1$  state) by 10%, and subsequently, it becomes nearly independent of the number of water molecules attached to salicylic acid.

For the second excited singlet state ( $S_2$ ), the transition dipole moment does not change with the addition of one water molecule, but it starts increasing with the addition of more water molecules and becomes a maximum at  $n = 3$ . Further addition of water molecules decreases the transition dipole moment dramatically. Therefore, the intensity of transition for the  $S_2$  state will be the largest for SA- $W_3$ . The origin of the unusual increase in transition dipole moment for  $n = 2$  and 3 is not clear.

The transition dipole moment for the third excited singlet state ( $S_3$ ) state shows an oscillatory behavior with the increasing number of water molecules in the complex. Addition of the first water molecule to salicylic acid decreases the transition dipole moment slightly, and then it increases and reaches a maximum for SA- $W_2$ . Addition of the third water molecule to the complex brings the transition dipole moment to a very low value, and then it increases on addition of the fourth and fifth water molecules. Addition of the sixth water molecule decreases the transition dipole moment but not as much as the addition of the third water molecule.

The  $\lambda_{\max}$  values for the first three excited singlet and triplet states of SA- $W_n$  are plotted as a function of  $n$  in Figure 8a. The predicted nominal shift (0.6 nm) in  $\lambda_{\max}$  for the  $S_1$  state, on addition of the first water molecule to SA, is in agreement with the experimental finding (1 nm) of Yahagi et al.<sup>7</sup> The change in  $\lambda_{\max}$  is nominal (in the range of 1–3 nm) for addition of up to three water molecules for all the states, whereas the addition of the fourth water molecule decreases  $\lambda_{\max}$  for the  $S_1$  and  $T_1$  states by  $\sim 17$  nm and for the  $T_2$  state by  $\sim 12$  nm and increases  $\lambda_{\max}$  for the  $S_2$  and  $S_3$  states by  $\sim 17$  nm (Table 3). Subsequently,  $\lambda_{\max}$  becomes nearly independent of the number of water molecules for all these states in the complex. The  $\lambda_{\max}$  value for the  $T_3$  state is almost independent of the number of water molecules in the complex. The sudden change in excitation energies on addition of the fourth water molecule could be attributed to differential stabilization of the ground and excited states of SA- $W_4$  arising from the extended proton dislocation in the system, which is not possible for  $n$  values up to 3. There is an overall blue shift (13 nm) in  $\lambda_{\max}$  for  $S_1$  state in going from  $n = 0$  (equivalent to nonpolar solvent) to  $n = 6$  (polar solvent) in qualitative agreement with the experimental

**TABLE 3: Wavelength (in nm) Corresponding to the Vertical Excitation Energies for S<sub>1</sub>, S<sub>2</sub>, S<sub>3</sub>, T<sub>1</sub>, T<sub>2</sub>, and T<sub>3</sub> States of Salicylic Acid–Water Complexes**

complex	S <sub>1</sub>	S <sub>2</sub>	S <sub>3</sub>	T <sub>1</sub>	T <sub>2</sub>	T <sub>3</sub>
SA	297.0	256.8	242.4	381.2	347.1	289.5
SA–W <sub>1a</sub>	296.4	251.1	238.1	379.0	346.4	289.0
SA–W <sub>2a</sub>	296.9	248.4	236.2	379.8	346.5	288.9
SA–W <sub>3a</sub>	293.9	246.4	237.0	373.2	347.2	287.8
SA–W <sub>4</sub>	280.9	262.3	248.3	357.4	337.1	285.2
SA–W <sub>5</sub>	285.5	260.6	246.3	362.7	340.5	286.1
SA–W <sub>6</sub>	284.2	251.1	244.5	360.9	339.4	285.1

results for SA in cyclohexane ( $\lambda_{\max} = 311$  nm) and water ( $\lambda_{\max} = 297$ ) (a blue shift of 14 nm).<sup>2,3</sup>

The energy of the different states of SA–W<sub>*n*</sub> complexes relative to the ground state of SA is plotted as a function of the number of water molecules in Figure 8b. It is clear that the order of energy of the states up to the addition of three water molecules is T<sub>1</sub> < T<sub>2</sub> < S<sub>1</sub> < T<sub>3</sub> < S<sub>2</sub> < S<sub>3</sub>. Further addition of water molecules to salicylic acid changes the energy order of states to T<sub>1</sub> < T<sub>2</sub> < T<sub>3</sub> < S<sub>1</sub> < S<sub>2</sub> < S<sub>3</sub>. There is an intersystem crossing between S<sub>1</sub> and T<sub>3</sub> states as the value of *n* changes from 3 to 4. This intersystem crossing is perhaps responsible for the fluorescence quenching of salicylic acid by water molecules.<sup>15</sup>

### Summary and Conclusion

The structure and stability of salicylic acid–water complexes have been investigated using DFT (B3LYP)/6-311++G(d,p) calculations. The vertical excitation energies and transition dipole moments for salicylic acid–water complexes have been computed using the TDDFT (B3LYP)/6-311++G(d,p) methodology. It is found that the hydrogen bond between carboxylic hydrogen and the oxygen of water is the strongest among all possible hydrogen bonds in the system. The hydrogen bond strength in these complexes is nearly additive. Change in  $\lambda_{\max}$  values for all the excited states studied is nominal (~1–3 nm) on addition of up to three water molecules. The addition of the fourth water molecule decreases  $\lambda_{\max}$  for S<sub>1</sub> dramatically, and for S<sub>2</sub> and S<sub>3</sub>  $\lambda_{\max}$  increases by nearly the same amount.  $\lambda_{\max}$  values for T<sub>1</sub> and T<sub>2</sub> follow the same trend as for S<sub>1</sub>, but for the T<sub>3</sub> state,  $\lambda_{\max}$  remains nearly independent of the number of water molecules in the complex. The transition dipole moment for the S<sub>1</sub> state changes nominally up to the addition of three water molecules, whereas the addition of the fourth water molecule brings it down by ~10%. For the S<sub>2</sub> and S<sub>3</sub> states, the transition dipole moment changes in an oscillatory manner with the number of water molecules in the complex. It has been

shown that there is an intersystem crossing between the S<sub>1</sub> and T<sub>3</sub> states with increasing *n*, which could be responsible for the observed fluorescence quenching of salicylic acid in water.

**Acknowledgment.** We are thankful to Dr. H. Mishra for valuable discussions. A.K.T. thanks the Council of Scientific and Industrial Research (CSIR), New Delhi, for a research fellowship. This study was supported in part by a grant from CSIR, New Delhi.

### References and Notes

- (1) Weller, A. Z. *Elektrochem.* **1956**, *60*, 1144; *Prog. React. Kinet.* **1961**, *1*, 187.
- (2) Pant, D. D.; Joshi, H. C.; Bisht, P. B.; Tripathi, H. B. *Chem. Phys.* **1994**, *185*, 137.
- (3) Joshi, H. C.; Mishra, H.; Tripathi, H. B. *J. Photochem. Photobiol., A: Chem.* **1997**, *105*, 15.
- (4) Joshi, H. C.; Tripathi, H. B.; Pant, T. C.; Pant, D. D. *Chem. Phys. Lett.* **1990**, *173*, 83.
- (5) Bisht, P. B.; Petek, H.; Yoshihara, K. *J. Chem. Phys.* **1995**, *103*, 5290.
- (6) Bisht, P. B.; Okamoto, M.; Hirayama, S. *J. Phys. Chem. B* **1997**, *101*, 8850.
- (7) Yahagi, T.; Fujii, A.; Ebata, T.; Mikami, N. *J. Phys. Chem. A* **2001**, *105*, 10673.
- (8) Sobolewski, A. L.; Domcke, W. *Chem. Phys.* **1998**, *232*, 257.
- (9) Maheshwari, S.; Chowdhury, A.; Sathyamurthy, N.; Mishra, H.; Tripathi, H. B.; Panda, M.; Chandrasekhar, J. *J. Phys. Chem. A* **1999**, *103*, 6257.
- (10) Sobolewski, A. L.; Domcke, W. *J. Phys. Chem. A* **2004**, *108*, 10917.
- (11) Mitsuzuka, A.; Fujii, A.; Ebata, T.; Mikami, N. *J. Phys. Chem. A* **1998**, *102*, 9779.
- (12) Lahmani, F.; Zehnacker-Rentien, A. *Chem. Phys. Lett.* **1997**, *271*, 6.
- (13) Abou El-Nasr, E. A.; Fujii, A.; Ebata, T.; Mikami, N. *Chem. Phys. Lett.* **2003**, *376*, 788.
- (14) Abou El-Nasr, E. A.; Fujii, A.; Yahagi, T.; Ebata, T.; Mikami, N. *J. Phys. Chem. A* **2005**, *109*, 2498.
- (15) Mishra, H.; Misra, V.; Mehata, M. S.; Pant, T. C.; Tripathi, H. B. *J. Phys. Chem. A* **2004**, *108*, 2346.
- (16) Kloppfer, W. *Adv. Photochem.* **1977**, *10*, 311.
- (17) Sandros, K. *Acta Chem. Scand., Ser. A* **1976**, *30*, 761.
- (18) Smith, K. K.; Kaufmann, K. J. *J. Phys. Chem.* **1981**, *85*, 2895.
- (19) Acuña, A. U.; Toribio, F.; Amat-Guerri, F.; Catalán, J. *J. Photochem.* **1985**, *30*, 339.
- (20) Acuña, A. U.; Amat-Guerri, F.; Catalán, J.; Gonzalez-Tablas, F. *J. Phys. Chem.* **1980**, *84*, 629.
- (21) Acuña, A. U.; Catalán, J.; Toribio, F. *J. Phys. Chem.* **1981**, *85*, 241.
- (22) Becke, A. D. *J. Chem. Phys.* **1993**, *98*, 1372.
- (23) Frisch, M. J.; et al. *Gaussian 03*, revision B.05; Gaussian, Inc.: Pittsburgh, PA, 2003.
- (24) Boys, S. F.; Bernardi, F. *Mol. Phys.* **1970**, *19*, 553.
- (25) Gora, R. W.; Grabowski, S. J.; Leszczynski, J. *J. Phys. Chem. A* **2005**, *109*, 6397.
- (26) Zhou, Z.; Shi, Y.; Zhou, X. *J. Phys. Chem. A* **2004**, *108*, 813.